EFFECT OF SUPERSOLIDUS LIQUID PHASE SINTERING ON THE MICROSTRUCTURE AND DENSIFICATION OF THE Al-Cu-Mg PRE-ALLOYED POWDER

H. Momeni[1], H. Razavi[1] and S. G. Shabestari[2*],

* *Shabestari@iust.ac.ir*

Received: Novamber 2010 **Accepted: April 2011**

[1] School of Metallurgy and Materials Engineering, Iran University of Science and Technology, Tehran, Iran.
[2] Center of Excellence for Advanced Materials Processing, Tehran, Iran.

Abstract: *The supersolidus liquid phase sintering characteristics of commercial 2024 pre-alloyed powder was studied at different sintering conditions. Pre-alloyed 2024 aluminum alloy powder was produced via air atomizing process with particle size of less than 100 μm. The solidus and liquidus temperatures of the produced alloy were determined using differential thermal analysis (DTA). The sintering process was performed at various temperatures ranging from the solidus to liquidus temperatures in dry N_2 gas atmosphere for 30 min in a tube furnace. The maximum density of the 2024 aluminum alloy was obtained at 610ºC which yields parts with a relative density of 98.8% of the theoretical density. The density of the sintered samples increased to the maximum 99.3% of the theoretical density with the addition of 0.1 wt. %Sn powder to the 2024 pre-alloyed powder. The maximum density was obtained at 15% liquid volume fraction for both powder mixtures.*

Keyword: *Al-Cu-Mg Aluminum Alloy, Supersolidus Liquid Phase sintering, Fractional grain boundary coverage, Densification*

1. INTRODUCTION

Sintering of aluminum is complicated by the presence of a thermodynamically stable oxide layer, which limits diffusion and hinders wetting and liquid spreading. More recently, significant improvements have been reported in the sinterability of aluminium alloys. Magnesium is known to react with the oxide and it therefore plays a major role in the sintering of aluminum [1]. The atmosphere is also known to be important and nitrogen is widely regarded as necessary [2,3]. It is widely known that the addition of traces of some elements can enhance the liquid phase's wettability which is favorable for a successful liquid phase sintering [3-10]. Most studies of the sintering characteristics of aluminum alloys focused on the liquid phase sintering of aluminum alloy blended powders [11-13] in which liquid phase sintering begins by mixing two or more powders of different compositions [14]. On heating, one powder melts or reacts with the other elements in the powder mixture to form a liquid between the particles that engulfs the more refractory phase. Fuentes et al used elemental aluminum powder that had mechanically alloyed and focused on the influence of processing variables upon structural characteristics and properties [15].

K. N. Ramakrishnan [16] investigated aluminum alloy made from atomized powder and found that the fine powder size distribution to be more desirable from the mechanical property point of view due to the retention of metastable phases.

Supersolidus liquid phase sintering (SLPS) is a variant of liquid phase sintering in which, pre-alloyed powders are heated between the solidus and liquidus temperatures of the alloy [17]. Liquid phase formed along the grain boundaries within the particles and so fragmented them into individual grains. The semisolid compact is densified as a result of capillary force exerted by the liquid film along the grain boundaries [14].

N. Showaiter and M. Youseffi [17, 18, 19] investigated the compaction, sintering, microstructure and mechanical properties of the commercial grade 6061 aluminium alloy powder with and without addition of elemental sintering aids such as lead (Pb), tin (Sn) or silver (Ag) and reported that additions of 0.1 and 0.4 wt% Sn or Ag, respectively, improved the sinterability of the elemental base powder with sintered densities of

96–98% theoretical. Ziani and Pelletier haven employed SLPS to 6061 aluminium pre-alloyed powder [20, 21]. Delgado et al [22] studied the effect of adding a eutectic Al–Si alloy to an Al–Cu alloy. Bishop et al investigated mechanical properties of 2014 aluminum pre-alloyed powder prepared using inert gas atomization [23] and reported that sintered densities for the commercial alloy were relatively unaffected by the presence of either Ag or Sn. There is few or no published paper which systematically describes the effects of Sn as a sintering aid additional element on the SLPS process of Al-Cu-Mg aluminum alloy. In this study, the effects of SLPS process on the microstructure and densification characteristics of the commercial 2024 aluminum pre-alloyed powder produced by air atomization with and without Sn addition have been investigated.

2. EXPERIMENTAL PROCEDURE

Pre-alloyed 2024 aluminum alloy powder was produced via air atomizing process. The chemical composition of the produced powder is given in Table 1. The atomized alloy powders were sieved by a sieve shaker. The size of powders used in the present study was less than 100 μm. Particle size distribution was determined by using particle size analyzer (PSA). Atomized powders were studied by means of scanning electron microscopy (SEM). 0.1 wt. % Sn powder with particle size of less than 71μm was used as a trace additive and mixed with the pre-alloyed powders in a turbula mixer for 30 min. The solidus and liquidus temperatures of the powder mixtures were determined by using differential thermal analysis (DTA). All DTA tests were performed at the heating rate of 10 ºC/min in helium gas atmosphere. The powders were compacted uniaxialy at pressure of 300 MPa in a cylindrical die having internal diameter of 12 mm. Oleic acid was used as die wall lubricant. The green density of the consolidated samples was calculated by measuring the sample weight and its geometrical dimensions with the accuracy of ±0.001 g and ±0.001 mm respectively .Samples were preheated for 20 min at 300ºC. The sintering process was performed at various temperatures ranging from the solidus to liquidus temperatures (580-620ºC) in a dry N_2 gas atmosphere for 30 min at a heating rate of 10ºC/min in a resistance tube furnace. The density of the sintered samples was measured through by Archimedes method. The microstructure of the samples was investigated using optical microscope and electron microscope (SEM) equipped with energy dispersive spectroscopy (EDS).

Table 1. Composition of pre-alloyed 2024 aluminum alloy (wt. %)

Al	Cu	Mg	Si	*Fe*	Mn
balance	3.95	1.23	0. 45	0.27	0.36

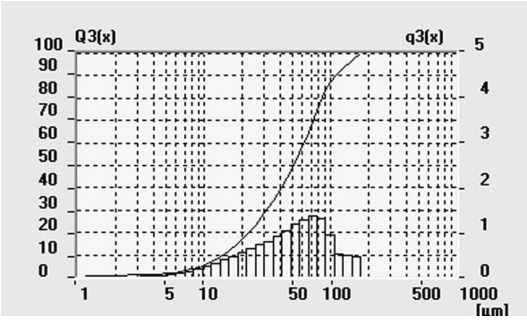

Fig. 1. Particle size distribution of the air atomized 2024 aluminum pre-alloyed powder

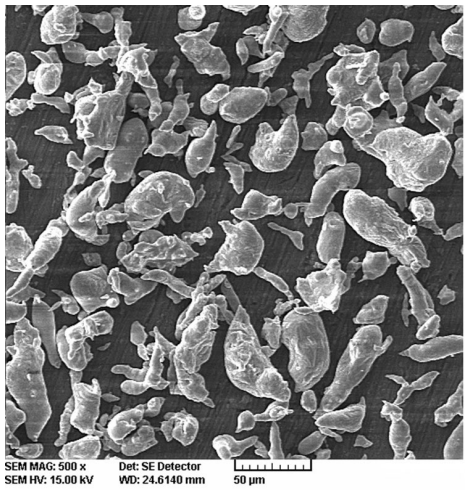

Fig. 2. SEM micrograph of the air atomized 2024 aluminum pre-alloyed powder

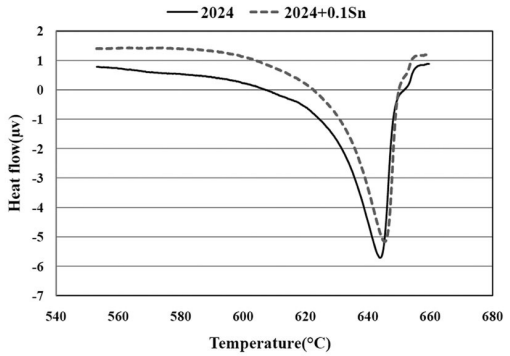

Fig. 3. DTA plot showing melting behavior of the air atomized 2024 aluminum alloy powder with and without Sn

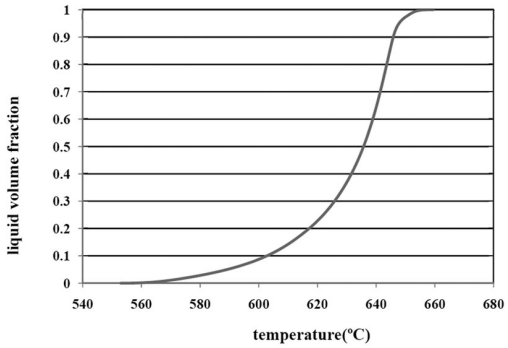

Fig. 4. Liquid volume fraction as a function of sintering temperature for air atomized 2024 aluminum alloy powder.

3. RESULTS AND DISCUSSION

Particle size distribution and SEM micrograph of the air atomized 2024 aluminum pre-alloyed powder are shown in Figures 1 and 2 respectively. It is seen that the powders have irregular shapes with the size less than 100 µm.

The DTA plot for the air atomized 2024 and 2024+0.1wt. % Sn aluminum alloy powders are shown in Figures 3. The onset of liquid formation in 2024 pre-alloyed powder occurred at 550 ºC and the powder melts completely at 660 ºC. Melting behavior of the air atomized 2024 aluminum alloy powder having 0.1 wt. % Sn is mostly the same as the samples having no tin. Therefore, Sn is not expected to increase the liquid volume fraction of the alloy significantly. The liquid volume fraction at a particular temperature above the solidus can be estimated by the ratio of the partial peak area to the total peak area of the DTA curve. This method of estimating the liquid volume fraction is believed to be within 10 pct of true volume fraction [24]. The liquid volume fraction was determined from Fig. 3 by using above method shown in Fig. 4. It seems that the liquid volume fraction increases from 3% at 580 ºC to 23% at 620 ºC.

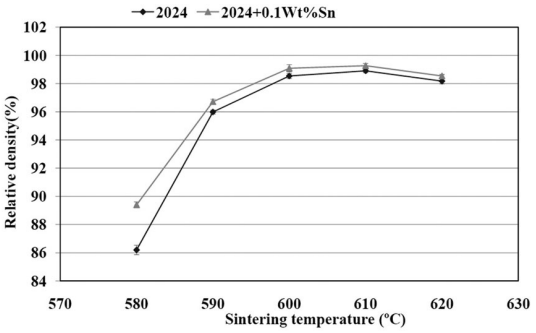

Fig. 5. Relative densities versus sintering temperature

Green density is obtained 89.4 % of theoretical density. Fig. 5 shows the changes of the relative density of each part sintered at temperatures

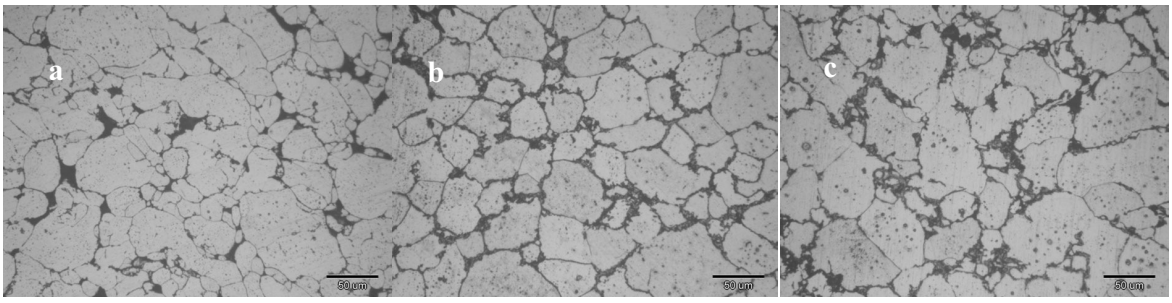

Fig. 6. Optical images of the sintered Al-2024 samples having 0.1 wt. % Sn at various sintering temperatures and water quenched a) 580 ºC, b) 600 ºC, c) 610 ºC

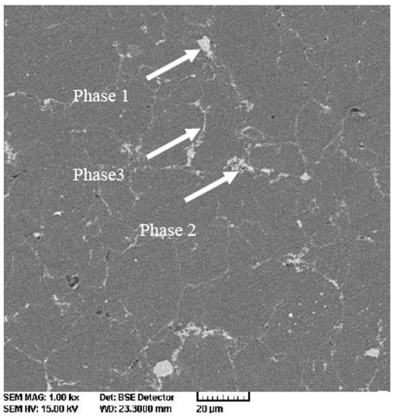

Fig. 7. BSE images of 2024 aluminum alloy sintered at 610ºC temperature and water quenched

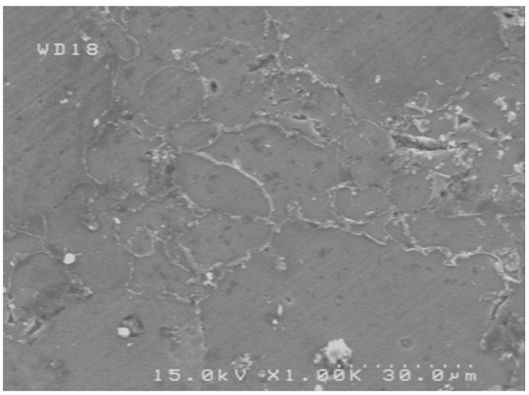

Fig. 8. BSE images of 2024 aluminum alloy sintered at 610ºC temperature and water quenched at higher magnificatio

ranging from 580 to 620 ºC. It can be seen from both density curves that sintered densities increase up to an optimum sintering temperature of 610 ºC. This process yielded parts with a maximum relative density of 98.8% for 2024 pre-alloyed Al powder and the sintered densities increased maximum to 99.3% with the addition of 0.1 wt. % Sn to the initial powder mixture.

The evolution of microstructure during sintering of the air atomized 2024 aluminum pre-alloyed powder with 0.1wt. %Sn is shown in Fig. 6. The microstructure of the samples sintered at 580 ºC is porous and the pores are distributed irregularly in the samples. Sintered parts start to be densified with increasing sintering temperature. The parts will be mostly full densified at the sintering temperature of 610 ºC.

Figures 7 and 8 show BSE images of 2024Aluminum alloy sintered at 610 ºC and then water quenched. The microstructure consists of á-Al grains surrounded by white phases. The width of the low melting point liquid film solidified at grain boundaries was measured from SEM image; which it was less than 1 micrometer. EDS analysis were performed on the phases that were formed at 610 ºC. The phases and their chemical compositions are shown in figure 9. Fig. 10 shows BSE image of the specimen having

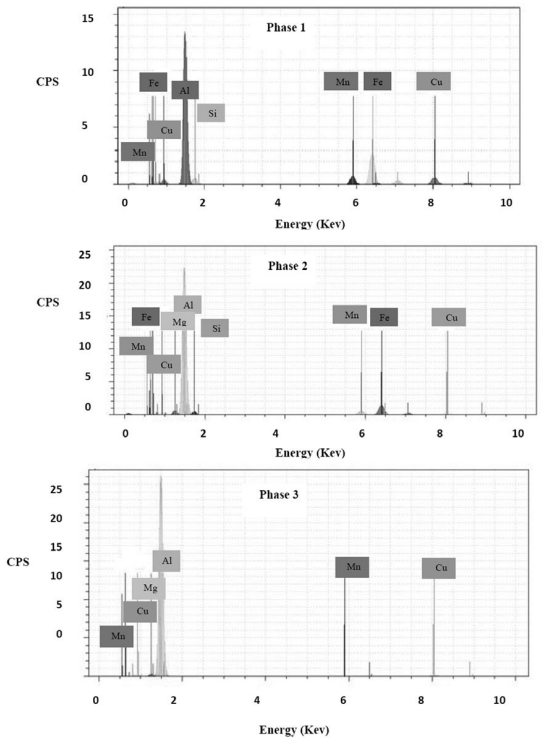

Fig. 9. EDS analysis of phases marked in Fig. 7

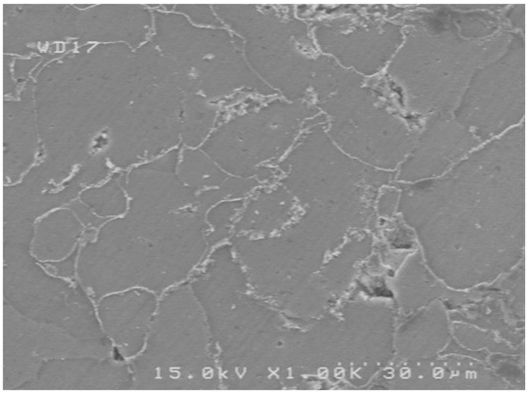

Fig. 10. BSE image of 2024 aluminum alloy having 0.1 wt. % Sn sintered at 610?C temperature and water quenched

0.1wt. %Sn, sintered at 610 ºC and then water quenched.

Microstructural evolution plays an important role in the density evolution during SLPS. It is necessary to understand the evolution of microstructure, and microstructural parameters to fully understand the mechanisms involved in densification during SLPS. The evolution of the microstructural parameters such as liquid volume fraction, contiguity, fractional liquid coverage, and grain size will be discussed.

Precipitation in Al–Cu–Mg–Si alloys is complex and a large variety of precipitated phases may be formed .The precipitates of any kinds (from binary and ternary phases, to complex quaternary phases and more) are found in these alloys. EDS analysis of these phases shown in the microstructure (Fig. 7) indicates that the boundary phases are composed of Al, Cu, Mg, Fe, Mn. The formation of the intermetallic compounds is due to the existence of trace amounts of Fe and Mn in the pre-alloyed powder. Eutectic structure containing intermetallic constituents have a low melting point.

With increasing sintering temperature to greater than solidus temperature these phases are seen in the form of a grain-boundary phase. It is apparent from the microstructures that the compacts sintered at high temperature exhibit a larger fraction of liquid phase (Fig. 6) .The effect of liquid volume fraction on the relative density of 2024 aluminum powder is shown in Fig. 11. The maximum density is obtained at 15% liquid volume fraction.

Contiguity (C_{SS}) is defined as the fraction of internal surface area of a phase shared with grains of the same phase in a dual phase microstructure. The fractional grain boundary coverage (FC) by the liquid defined as: $FC=1-C_{SS}$ [14]. Contiguity can be calculated by counting the number of solid-solid (N_{SS}) and solid-liquid (N_{SL}) interfaces intersected by random lines superimposed on the microstructure using the Eq. 1:

$$C_{SS} = \frac{2N_{SS}}{N_{SL} + 2N_{SS}} \quad (1)$$

The fractional grain boundary coverage for the air atomized 2024 aluminum alloy and 2024+0.1wt. % Sn aluminum alloy powders as a function of liquid volume fraction are shown in Fig. 12. The fractional grain boundary coverage by liquid was increased with increasing liquid volume fraction in the microstructure. The amount of liquid phase required for densification was reduced by the formation of a continuous liquid film along the grain boundaries. As seen in Fig. 5, the density of the sintered samples increases rapidly due to particle rearrangement and bulk shrinkage that were progressed by the supersolidus liquid phase which formed at 610ºC. An excess amount of liquid phase forms with increasing the temperature to sintering temperatures greater than 610 ºC. Therefore, it results in grain coarsening (Fig. 13), pore coalescence and so reduction of relative density (Fig. 5).

Additions of 0.1wt. %Sn, improved the density of the 2024 Al alloy. Tin is an important sintering

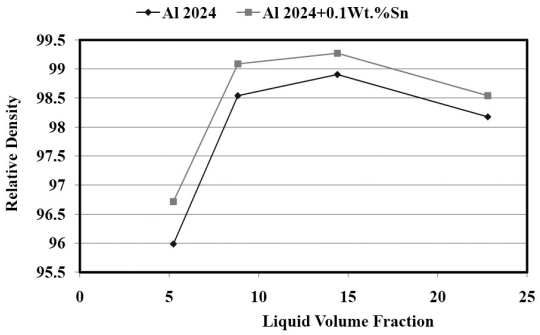

Fig. 11. Relative density as a function of liquid volume fraction for the Al 2024 and Al 2024+0.1 wt. % Sn

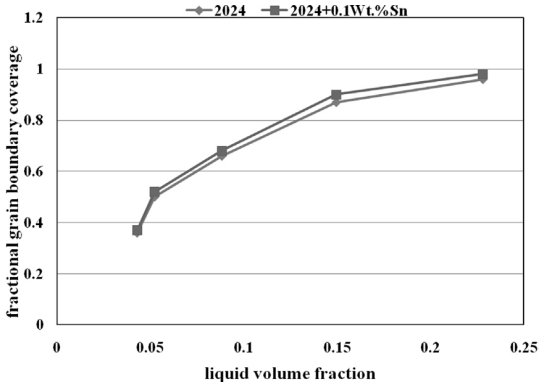

Fig. 12. Fractional grain boundary coverage as a function of liquid volume fraction for Al 2024 and Al 2024+0.1 wt. % Sn

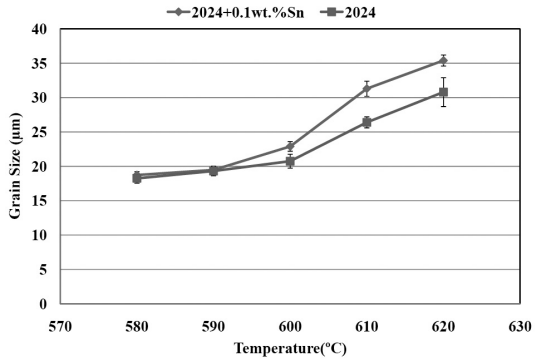

Fig. 13. Grain size as function of sintering temperatures for Al 2024 and Al 2024+0.1 wt. % Sn

activator under nitrogen. Tin has a higher vacancy binding energy and a higher diffusivity in Al than Cu does [9]. It is possible that tin binds with the vacancies in the Al, thereby reducing the rate of Cu diffusion in the Al [9]. This would hinder the dissolution of copper and hence delay the transient aspect of the system. In this state the liquid phase persists for longer times, and so improves the fractional grain boundary coverage (Fig. 13). The dihedral angle φ defines the ability of the liquid to penetrate the grain boundaries. An estimation of the dihedral angle based has been given as Eq. 2 [25]:

$$F_C = 2.64\left(\frac{V_L}{K}\right)^{\frac{1}{2}} \tag{2}$$

Where Fc is the fractional liquid coverage, V_L is the liquid volume fraction. The term K depends only on the dihedral angle φ and is given by Eq. 3:

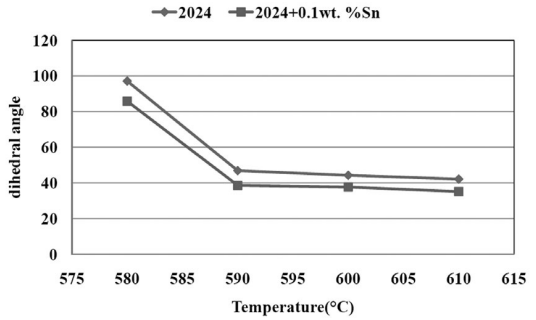

Fig. 14. Dihedral angle as function of sintering temperatures for Al 2024 and Al 2024+0.1 wt. % Sn

$$k = \sqrt{3} + \frac{3}{\tan(30 - (\frac{\varphi}{2}))} - \left[\frac{30 - (\frac{\varphi}{2})}{60}\right] \frac{\pi}{\sin^2(30 - \frac{\varphi}{2})} \tag{3}$$

Based on the above equation are calculated the dihedral angle for 2024 and 2024 with 0.1wt. % tin (Fig. 14)

It is noted that with increasing sintering temperature, dihedral angle was decreased and tin improved wetability and reduced dihedral angle. With decreasing dihedral angle, surface energy required to cause grain boundary penetration reduced by Eq. 4 [26].

$$-\frac{d\gamma_{SL}}{\gamma_{SL}} = \frac{\varphi}{2}\tan(\frac{\varphi}{2}) \tag{4}$$

Without tin, aluminium nitride forms on the liquid at the liquid-vapor interface, which alerts the wetting conditions to the detriment the sintering. With addition of Sn, slow and controlled nitridation occurs and because of the low surface tension of the Sn, the wetting of the infiltrant improves and increases the infiltration rate. Therefore, it improves the fractional grain boundary coverage and densification.

5. CONCLUSIONS

Based on the results obtained in this research, the following conclusions can be stated:

1. Rapid increase in density was resulted from particle rearrangement and bulk shrinkage induced by the formation of supersolidus liquid phase at 610 ºC.
2. The maximum density in 2024 pre-alloyed Al powder was obtained at 610 ºC. This process yielded parts with a relative density of 98.8% of the theoretical density.
3. The fractional grain boundary coverage by liquid improved with the addition of 0.1 wt. %Sn, and densities increased to 99.3% of the theoretical density after sintering.
4. Maximum density is yielded at 15% liquid volume fraction.
5. With increasing sintering temperature, dihedral

angle for 2024 aluminium pre-alloyed powder was decreased and tin improved wetability and reduced dihedral angle.

6. Grain coarsening, pore coalescence and therefore, reduction in relative density occur with increasing the temperature to greater than 610 ºC.

REFERENCES

1. Kondoh, K., Kimura, A., and Watanabe, R., "Effect of Mg on Sintering Phenomenon of Aluminium Alloy Powder Particle", Powder Metall , 2001, 44(2), 161-164
2. Pieczonka, T., Schubert, Th., Baunack, S. and Kieback, B., "Dimensional Behavior of Aluminum Sintered in Different Atmospheres", Mater. Sci. Eng. A, 2008, 478, 251.
3. Schaffer, G. B., Yao, J. Y., Bonner, S. J., Crossin, E., Pas, S. J. and Hill, A. J., "The effect of tin and nitrogen on liquid phase sintering of Al–Cu–Mg–Si alloys", Acta Mater, 2008, 56, 2615.
4. Schaffer, G. B., Huo, S. H., Drennan, J. and Auchterlonie, G. J., "The Effect of Trace Elements on the Sintering of an Al–Zn–Mg–Cu Alloy", Acta Mater, 2001,49, 2671.
5. Bishop, D. P., Li, X. Y., Tandon, K. N. and Caley, W. F., "Dry Sliding Wear Behaviour of Aluminum Alloy 2014 Microalloyed With Sn and Ag", Wear, 1998, 222, 84.
6. Kent, D., Schaffer, G. B. and Drennan, J., "Age Hardening of a Sintered Al–Cu–Mg–Si–(Sn) Alloy", Mater. Sci. Eng. A, 2005, 640, 55-73.
7. Kondoh, K., Kimura, A. and Wataabe, R., "Effect of Mg on Sintering Phenomenon Of Aluminum Alloy Powder Particle", Powder Metall, 2001, 44(2), 161.
8. Mcphee, W. A. G., Schaffer, G. B. and Drennan, J., "The Effect of Iron on Liquid Film Migration and Sintering of an Al–Cu–Mg Alloy", Acta Mater, 2003, 51, 3701.
9. Sercombe, T. B. and Schaffer, G. B., "The Effect of Trace Elements on the Sintering of Al-Cu Alloys", Acta Mater, 1999, 47, 689.
10. Sercombe, T. B. and Schaffer, G. B., " On the Use of Trace Additions of Sn to Enhance Sintered 2xxx Series Al Powder Alloys", Mater. Sci. Eng. A, 1999, 268, 32.
11. Min, K. H., Kang, S. P., Lee, B. H., Lee, J. K. and Kim, Y. D., "Liquid Phase Sintering of the Commercial 2xxx Series Al Blended Powder", J. Alloys. Compd, 2006, 419, 290.
12. Schaffer, G. B., Sercombe, T. B. and Lumley, R. N., "Liquid Phase Sintering of Aluminium Alloys", Mater. Chem. Phys, 2001, 67, 85.
13. Martin, J. M. and Castro, F., "Liquid Phase Sintering of P/M Aluminium Alloys: Effect of Processing Conditions", J. Mater. Process. Tech, 2003, 143–144, 814.
14. German, R. M., "Sintering theory and practice", Wiley, New York, 1996
15. Fuentes, J. J., Rodriguez, J. A. and Herrera, E. J., "Processing of mechanically alloyed aluminum powder: a metallographic study", Mater Charact, 2010, 61, 386.
16. Ramakrishnan, K. N., "Investigation of the Effect of Powder Particle Size Distribution on the Powder Microstructure and Mechanical Properties of Consolidated Material Made From a Rapidly Solidified Al-Fe-Ce Alloy Powder. Part I. Powder Microstructure", Mater Charact, 1994, 33, 119.
17. Showaiter, N. and Youseffi, M., "Compaction, Sintering and Mechanical Properties of Elemental 6061 Al Powder With and Without Sintering Aids", Materials and Design, 2008, 29, 752.
18. Youseffi, M. and Showaiter, N., Martyn, Mt., "Sintering and Mechanical Properties of Prealloyed 6061 Al Powder With and Without Common Lubricants and Sintering Aids", Powder Metall, 2006, 49(1), 86.
19. Youseffi, M. and Showaiter, N., "P/M Processing of Elemental and Prealloyed 6061 Aluminium Alloy With and Without Common Lubricants and Sintering Aids", Powder Metall, 2006, 49(3), 240.
20. Ziani, A. and Pelletier, S., "Supersolidus Liquid-Phase Sintering Behavior of Degassed 6061 Al Powder", Int J Powder

Metall, 1999, 35(8), 49.
21. Ziani, A. and Pelletier, S., "Sintered 6061 Al Pre-Alloyed Powder: Processing and Mechanical Behaviour", Int J Powder Metall, 1999, 35(8), 59.
22. Delgado, M. L., Ruiz-Navas, E. M., Gordo, E. and Torralba, J. M., "Enhancement of Liquid Phase Sintering Through Al–Si Additions to Al–Cu Systems" J. Mater. Process. Tech, 2005, 162–163, 280.
23. Bishop, D., Cahoon, J. R., Chaturvedi, Mc. Kipouros, G. J. and Caley, W. f., "On Enhancing the Mechanical Properties of Aluminium P/M Alloys", Mater. Sci. Eng A, 2000, 29(1–2), 16.
24. Lal, A., Iacocca, R. G. and German, R. M., "Densification During the Supersolidus Liquid Phase Sintering of Nickel-Based Prealloyed Powder Mixtures", Metall. Mater. trans A, 1999, 30A, 2201.
25. Liu, J., Lal, A. and German, R. M., "Densification and Shape Retention in Supersolidus Liquid Phase Sintering", Acta. Mater, 1999, 47(18), 4615.
26. Aksay, I. A., Hoge, C. E. and Pask, J. A., "Wetting under Chemical Equillibrium and Nonequillibrium Conditions", J. Phys. Chem, 1974, 78(12), 1178.